

Conductivity anisotropy and transverse magnetoresistance of NbSe₃

N. P. Ong and J. W. Brill

Department of Physics, University of Southern California, Los Angeles, California 90007

(Received 10 July 1978)

The first-transverse dc conductivity measurements on a member of the transition-metal trichalcogenides (NbSe₃) are presented. The conductivity anisotropy σ_b/σ_c (where b is the chain axis) was obtained using the Montgomery technique, and varies from 10 to 20 as a function of temperature. The transverse resistivity ρ_c also shows anomalies associated with the charge-density-wave transitions at T_1 (142 K) and T_2 (58 K). However, these anomalies are smaller than the corresponding ones in ρ_b . The quantity $R_H(0)/(\rho_b \rho_c)$, where R_H is the Hall constant, demonstrates explicitly the freeze-out of thermally excited quasiparticles below each transition. We show that at both transition gaps appears on the hole surface, and the hole concentration decreases rapidly. The transverse magnetoresistance at low fields has also been measured. Its monotonic power-law decrease with increasing temperature shows explicitly that the resistivity anomalies are due to changes in the carrier concentration, and not in the lifetimes.

I. INTRODUCTION

The transition-metal chalcogenides have proved to be a remarkably fertile series of compounds for the study of instabilities of the electron gas of reduced dimensionality. The MX_2 (where M is a transition metal element and X is one of the chalcogens) compounds form layered structures¹ and the electron gas has a quasi-two-dimensional character. A host of phase transitions into the incommensurate charge-density-wave (ICDW) and commensurate charge-density-wave state (CCDW) occurs in the various poly-types of these compounds. Much theoretical effort has been expended to study the nature of the incommensurate phase and how an ICDW "locks-in" to the underlying host lattice. For instance, McMillan² has proposed that the ICDW state in 2H-TaSe₂ is in fact one in which the charge-density-wave (CDW) achieves commensurability over microdomains which are separated by domain walls (discommensurations) where the CDW phase undergoes an abrupt change. It remains unclear whether such discommensurations or similar defects occur also in other ICDW systems such as 2H-NbSe₂, or whether the canonical CDW theory of Chan and Heine³ is adequate.

In the last two years compounds of the type MX_3 have been shown to exhibit the same kinds of electronically driven instabilities. Specifically, the compounds NbSe₃,^{4,5} NbS₃,⁶ TaSe₃,^{5,7} and ⁸TaS₃ have been synthesized and studied. The occurrence of CDW's in the MX_3 family is significant because the members generally have a linear-chain structure with high conductivity along the chain direction. In contrast to the layered structure of the MX_2 family where the high conductivity occurs

in the basal plane, the MX_3 metals could possibly show quasi-one-dimensional behavior. Indeed, Sambongi *et al.*,⁷ have shown that TaS₃ undergoes a transition into the insulating CCDW state, similar to the well-studied quasi-one-dimensional conductors, tetrathiafulvalene tetracyanoquinodimethane⁹ (TTF-TCNQ) and the mixed-valence compounds⁹ KCP and their numerous derivatives. Another member TaSe₃, shows metallic behavior⁵ at all temperatures down to 2.2 K where it becomes superconducting.⁸ No superlattice formation has been reported for TaSe₃.

In many ways the most interesting member of the MX_3 family is NbSe₃ which was first structurally characterized by Meerschaut and Rouxel.⁴ Monceau and co-workers,⁵ first showed the occurrence of two giant resistivity anomalies associated with phase transitions at T_1 (~142 K) and T_2 (58 K) which they inferred to be CDW transitions, from the pressure dependence¹⁰ of T_1 and T_2 . Support for this hypothesis was provided by measurements on the Hall effect¹¹ and Young's Modulus¹² which showed respectively a loss of carriers at both T_1 and T_2 , and an elastic anomaly at T_1 . Furthermore, the growth of a gap at the Fermi surface (FS) at both transitions was inferred¹³ by applying the BCS gap equation to data obtained from the non-Ohmic measurements of the longitudinal conductivity. Since then other groups¹⁴⁻¹⁶ have obtained direct superlattice evidence of ICDW's in both low-temperature phases by electron diffraction and x-ray studies.

The confirmation of the CDW state in NbSe₃ is significant because of the anomalous-electronic transport properties which occur below T_1 . The giant resistivity anomalies show non-Ohmic breakdown effects¹⁷ under weak dc electric fields.

The conductivity also shows¹⁸ strong frequency dependence in the gigahertz region even when the ac field is much weaker than the value required to observe non-Ohmic behavior at zero frequency. The great difficulties in accommodating these results within the framework of a single-particle picture have been discussed in Refs. 13 and 18. In these papers it was also suggested that the significant enhancement of the conductivity may arise from the depinning of the rigid CDW condensate which is then accelerated by the E field. This possibility has been discussed by many workers^{19,20} in the context of one-dimensional "Fröhlich superconductivity." Bardeen²¹ recently applied the two-fluid model to account for the temperature dependence of the activation field in NbSe_3 , and finds that the depinning field should first decrease, then increase as the temperature decreases, in qualitative agreement with the experiment. However, little else is understood, especially quantitatively, regarding the anomalous transport behavior aside from the strong suspicion that a collective mode of the CDW condensate is being excited.

In this paper we present results on the galvanomagnetic and other transport properties of NbSe_3 in the zero-frequency-Ohmic regime, restricting current values to below the Ohmic breakdown values. Although the nature of the current-carrying excitations in the non-Ohmic and/or high-frequency regime is of paramount interest, the understanding derived from the analysis of the galvanomagnetic and conductivity anisotropy data in the Ohmic region is a necessary first step towards an understanding of the anomalous behavior. It will be seen in the following paper²² (II) that the various transport measurements taken together offer a rather complete view of the normal uncondensed electrons and holes in this metal. The galvanomagnetic measurements in the high-frequency and high electric field regimes are currently in progress and will be reported in a later publication.

Hall measurements on NbSe_3 from 2 to 300 K, with the B field along a^* and the current parallel to b (the chain axis) have been reported by Ong and Monceau¹¹ (OM). Monceau²³ has measured the Shubnikov-de Haas oscillations in the magnetoresistance. Fleming, Polo, and Coleman²⁴ (FPC) have also reported oscillatory magnetoresistance measurements in NbSe_3 and TaSe_3 , as well as high-magnetic-field Hall measurements in NbSe_3 . A more complete mapping of the Shubnikov frequencies has recently been obtained by Monceau and Briggs²⁵ (MB). The preceding measurements are all in substantial quantitative agreement except for the disagreement on Hall

polarity reported by OM and FPC. Together with the conductivity anisotropy in the b - c plane and the transverse low-field magnetoresistance measurements to be reported here one should have sufficient data to unravel the contributions from the electron and hole pockets. In particular one would hope for a direct observation of the loss of carriers near the CDW transitions, as thermally excited quasiparticles across the developing gaps are frozen out with decreasing temperature. Evidence for this behavior is obtained by combining the Hall and anisotropy measurements. A full analysis of the galvanomagnetic data is presented²² in II.

II. EXPERIMENTAL DETAILS

Conductivity anisotropy measurements were done using the Montgomery²⁶ technique. The fibrous morphology of the crystals and the minute transverse dimensions presented the most serious difficulties in measuring the dc transverse conductivity. Samples were mounted on a sapphire substrate and glued to the substrate by four silver paint (du Pont 4922) droplets, which also served as contacts for the gold leads. This mounting configuration is less satisfactory in one respect than some that have been reported²⁷ in the literature. The differential contraction of the sample and substrate sets up stresses in the sample which lead to cracks parallel to the chain axis. These stress-induced cracks show up as irreproducible jumps in the measured transverse conductivity. Nonetheless, this mounting configuration was used because one could achieve better control over the size of the contacts to the sample. Attempts to use techniques such as that described by Coleman²⁷ resulted in the droplets completely enveloping the thin sample. The Montgomery configuration requires the contacts to be at the four corners of a rectangular sample. Because the ends of single crystals tend to be frayed the contacts were placed approximately $\frac{1}{2}$ mm away from the ends. Since the transverse dimension in the c direction was typically 300 μm and the diameter of the paint droplets was at least 100 μm great care was required to avoid shorting out contacts on opposite sides of the sample. The technique which proved most successful was to place the sample on the substrate and to wash it with a drop of butyl acetate. This improved adhesion of the sample to the substrate as well as the contact between the sample and paint. When the butyl acetate had evaporated a small droplet of paint was placed on the substrate close to the sample and edged in with a 3-mil wire until contact was achieved. The optimum viscosity was maintained

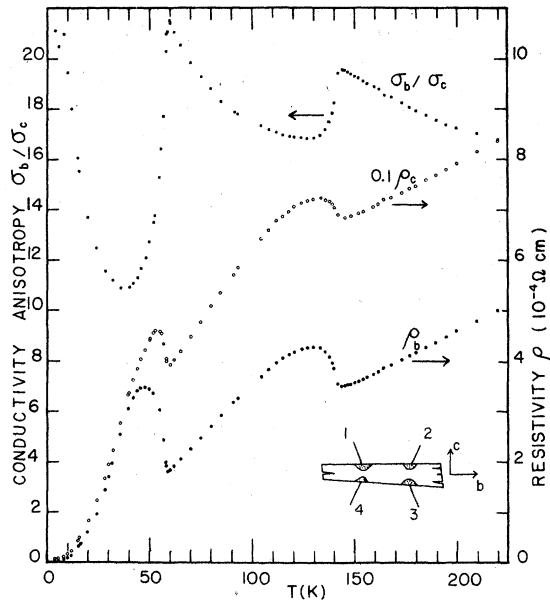


FIG. 1. Conductivity anisotropy (in the b - c plane), the transverse resistivity, and the longitudinal resistivity of NbSe_3 (in descending order). The transverse resistivity has been reduced by a factor of 10 for convenience. The longitudinal resistivity profile is in good agreement with previous results obtained by the conventional four-probe technique. Like ρ_b , the transverse resistivity ρ_c is also greatly perturbed by the CDW transitions at T_1 and T_2 . The inset shows the actual sample orientation in the Montgomery technique used.

by diluting a fresh "pot" of paint with butyl acetate for each contact. To ensure that the sample could withstand the stresses associated with cooling only those crystals with substantial thickness a in the a^* direction (normal to substrate) were used. A successful cool down was judged to be one in which no measurable hysteresis was observed on subsequent warm up. The amount of stress could also be estimated by comparing T_1 and T_2 as well as the size of the two anomalies in the longitudinal resistivity with the ambient pressure results. Chaussy *et al.*¹⁰ have shown that these parameters are sensitive to applied hydrostatic pressure. In the results reported here the longitudinal resistivity and the transition temperatures show no measurable difference from the ambient pressure results. Thus we may safely ignore the effect of these stresses. The substrate was thermally anchored to a copper platform which was surrounded by He gas and enclosed in a double-vacuum jacket. Thermal stability was maintained to ± 10 mK while the two measurements were made. The sample whose

conductivity anisotropy is shown in Fig. 1 had dimensions $1980 \times 290 \times 50 \mu\text{m}$. Since the contact dimensions varied from 30 to $50 \mu\text{m}$ there is some uncertainty over what the appropriate effective ratio of the sides of the crystal b/c should be. This is discussed in Sec. III.

For the transverse magnetoresistance measurements much thinner fibers can be used (typically $20\text{-}\mu\text{m}$ wide). Leads were mounted in the conventional four-probe configuration with the B field along the a^* axis and the current in the b direction. A quadratic fit to the resistivity at low fields was made at each temperature. This is important below ~ 12 K where the resistivity starts deviating from quadratic behavior at relatively low fields. The low-field magnetoresistance $\Delta\rho/\rho_0 B^2$ where ρ_0 is the zero-field resistivity is very large at 4.2 K (corresponding to an equivalent mobility of $\sim 40000 \text{ cm}^2/\text{V sec}$), but rapidly decreases to an equivalent mobility of $200 \text{ cm}^2/\text{V sec}$ at 55 K. No magneto-resistance could be measured to our sensitivity at fields of 70 kG above the T_2 transition. Our highest temperature data is at 55 K. At 15 kG the measured fractional change in the resistivity at 55 K is 7×10^{-4} . Since the temperature-coefficient of the resistivity is very large at this temperature $\rho^{-1} d\rho/dT \approx -8 \times 10^{-2} \text{ K}^{-1}$ the fractional increase in ρ would be suppressed by a temperature drift of 9 mK during the time of the field sweep. This represents an upper limit on the cryogenic stability of our apparatus. The temperature of the sample chamber was controlled by a capacitance sensor which, unfortunately, was least sensitive around 60 K. Transients caused by the switching relays in the magnet supply were suppressed by careful screening of the sample leads. Altogether data from three samples were taken. Despite the scatter they are in reasonable agreement with each other.

III. RESULTS AND ANALYSIS

In Montgomery's²⁶ technique for measuring the conductivity anisotropy of a rectangular sample of sides b and c , the potential drop V_b across contacts 3 and 4 (see Fig. 1) is first measured with the current I going through contacts 1 and 2. Next, the potential drop V_c across contacts 2 and 3 are measured with the same current going through contacts 1 and 4. Specializing to the case where the third dimension a (along the a^* axis) is negligible compared to c , Montgomery and Logan *et al.*²⁸ show that the resistivity in the b and c directions are given by

$$\rho_b = H(x)a(V_c/I)(cx/b), \quad (1)$$

$$\rho_c = H(x)a(V_c/I)(b/cx), \quad (2)$$

where

$$H(x) \equiv \frac{\pi}{4} \ln \frac{1+2q+2q^4 \dots}{1-2q+2q^4 \dots}, \quad q \equiv e^{-\pi x}, \quad (3)$$

and x is the solution to the equation

$$r \equiv \frac{V_b}{V_c} = \frac{\{\pi x/4 - \ln[2(1-q^2+q^6)/(1+2q+2q^4)]\}}{\{\ln[(1+2q+2q^4)/(1-2q+2q^4)]\}}. \quad (4)$$

In practice at each temperature the ratio r is formed from the measured V_b and V_c . Equation (4) is then solved for x , and H computed from Eq. (3). Substitution into Eqs. (1) and (2) gives ρ_b and ρ_c . For reference we note that the product

$$\rho_b \rho_c = H(x)^2 a^2 (V_c/I)^2 \quad (5)$$

is independent of b/c . To solve Eq. (4) for x we have found it convenient to use the following series which gives an accuracy of $\pm 0.01\%$ when $1 < r < 30$:

$$x = A + B \ln r + C (\ln r)^2 + D (\ln r)^3 \dots \quad (6)$$

$A = 0.997229$, $B = 0.160697$, $C = 1.231448 \times 10^{-2}$, $D = -3.79740 \times 10^{-4}$.

Figure 1 shows the computed anisotropy in the b - c plane and the separate resistivities along the two axes. (The transverse resistivity ρ_c has been reduced by a factor of 10.) As mentioned in Sec. I the longitudinal anomaly sizes in ρ_b show good agreement with conventional four-probe measurements on single ribbons. Furthermore, the room temperature value of ρ_b ($655 \mu\Omega \text{ cm}$) is in good agreement with previously reported⁵ measurements. A rather surprising feature of the transverse resistivity ρ_c is the sizeable anomaly at T_1 . This is unexpected from the orientation of the superlattice Bragg plane which is normal to the b axis. Equally unexpected is the fact that the appearance of the CDW at T_2 which has spanning vector¹⁵ (0.5, 0.26, 0.5) seems to disrupt ρ_c less than ρ_b . Below T_2 the transverse resistivity ρ_c decreases much more rapidly than ρ_b but at liquid-helium temperatures the anisotropy has returned to the value it had at 59 K. As mentioned before, the computed anisotropy ρ_c/ρ_b is very sensitive to the choice of the ratio of the sides b/c . Since the contacts have finite size it is not clear what values for b/c is appropriate. The anisotropy shown in Fig. 1 (~ 16 at 290 K) was computed with a value of b/c equal to 5.0. Room-temperature measurements on two other samples gave values of ρ_c/ρ_b which varied between 10 and 30, again depending on the choice of b/c . Thus the absolute value of the anisotropy is known only to $\pm 50\%$. Nonetheless it may be seen from Eqs.

(4) and (5) that the value of x and $(\rho_b \rho_c)$ are unaffected by this uncertainty. It will turn out that in analyzing the anisotropy data in conjunction with the galvanomagnetic data the important quantity is $\rho_b \rho_c$ which does not depend on b/c . The quantity that figures prominently in these analyses is $R_H/\rho_b \rho_c$ which may be shown to be independent of all sample dimensions. (Both R_H and $\rho_b \rho_c$ are linear in a .) Similarly the magnetoresistance is independent of sample dimensions.

Knowing the product $\rho_b \rho_c$ (solid circles in Fig. 2), enables us to proceed one more step in understanding the Hall effect of NbSe_3 . The puzzling feature of the Hall constant at zero field, $R_H(0)$, is the large increase in $|R_H(0)|$ below T_1 and T_2 . Specifically¹¹ $|R_H(0)|$ undergoes an eightfold increase as the temperature decreases from 145 to 60 K and appears to be still increasing when the T_2 transition is reached. A similar large increase (12-fold) occurs below the T_2 transition (between 59 and 36 K). In a one-band model $R_H(0)$ is in-

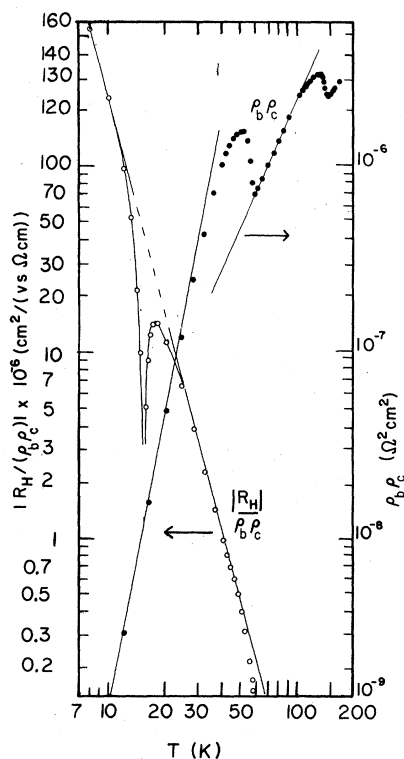


FIG. 2. Product of the resistivities $\rho_b \rho_c$ (solid circles) and the absolute value of the quantity $A \equiv R_H(0)/\rho_b \rho_c$ (open circles) vs temperature in log-log scale. The "resonance" structure in $|A|$ is due to the zero crossing of $R_H(0)$ at 15 K. The straight line through the open circles reflects the dominant power-law behavior $T^{-\alpha}$ of the mobilities.

versely proportional to the carrier concentration. However, it is clear that such large increases in $R_H(0)$ with no sign of saturation is incompatible with this simple interpretation, since the resistivity shows only a 20% and 50% change at T_1 and T_2 , respectively. Nevertheless, one would hope that the Hall data would be amenable to a reasonably straight-forward interpretation, and provide experimental evidence of loss of carriers as required by the canonical CDW theory.³ The change of sign of $R_H(0)$ at 15 K indicates that a two-band model is appropriate for NbSe₃. This is also consistent with the very large transverse magnetoresistance observed at low temperatures. The expression for the Hall constant at zero field for the two-band model (assuming a closed simply-connected FS for both holes and electrons) is given by²²

$$R_H(0) = - (n\mu_1\mu_2 - p\nu_1\nu_2) / e(n\mu_1 + p\nu_1)(n\mu_2 + p\nu_2), \quad (7)$$

where e is the magnitude of the electronic charge, $n(p)$ are the electron (hole) density, $\mu_1(\mu_2)$ is the electron mobility in the $x(y)$ direction and ν_1, ν_2 are the analogous hole mobilities. The form of the denominator suggests that a simpler expression is obtained by dividing Eq. (7) by $(\rho_x\rho_y)$. This gives

$$A \equiv R_H(0) / \rho_x\rho_y = e(p\nu_1\nu_2 - n\mu_1\mu_2), \quad (8)$$

whose absolute value is plotted in Fig. 2 (open circles) in log-log scale. It becomes immediately apparent that the temperature dependence of A is dominated by that of the mobilities (lifetimes of carriers) which have a power-law dependence. Dividing out this power-law dependence we thus isolate the temperature variation predominantly due to n and p . In Fig. 3 the quantity $A(T)(T/T_2)^{3.875}$ is shown versus temperature. The deviation above 40 K of A from the straight line in Fig. 2 now manifests itself as a sharp change in the hole concentration relative to the electron concentration. To be consistent with the conventional concepts of gap formation at the FS we postulate from Fig. 3 that the gapping occurs at the hole surface. This is because $(p\nu_1\nu_2 - n\mu_1\mu_2)(T/T_2)^{3.875}$ increases algebraically as T_2 is approached from below.

(The reader may question our treatment of the Hall effect due to the thermally excited quasiparticles. On the hole FS the excitation of holes across the CDW gap leaves vacancies behind which are electronlike. These will presumably contribute a negative Hall signal, and to a first approximation, cancel the Hall signal from the excited holes. However, this argu-

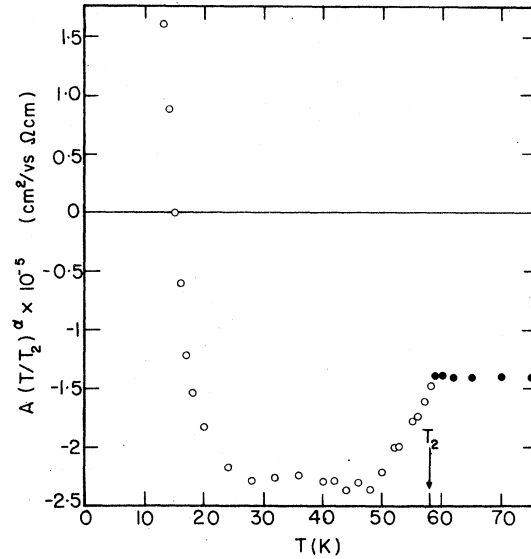


FIG. 3. Temperature dependence of A with the power-law dependence $T^{-\alpha}$ divided out. Below T_2 (open circles) α equals 3.875. Above T_2 (solid circles) α has the value 2.792. It is argued in the text that the increase in A as the temperature increases towards T_2 is due to the thermal excitation of quasi-particles across the CDW gap.

ment is incorrect. By studying the topology of the constant energy surfaces it may be shown that the vacancies will always have the same galvanomagnetic response as the excited quasiparticles. A more detailed treatment is offered elsewhere.) Much the same analysis can be applied to the Hall data above T_2 . Again we find that A vs T in a log-log scale falls on a straight line of slope -2.792 except near T_1 . Dividing out this power-law dependence shows the same carrier freeze-out phenomenon below T_1 (see Fig. 4) rather more clearly than in Fig. 3 because $R_H(0)$ has no zero crossing above T_2 . Above T_1 , $A(T/T_1)^{1.744}$ is temperature independent indicating no relative changes in the electron and hole concentrations. Thus the slight decrease in $R_H(0)$ above 145 K that is evident in Fig. 3 of Ref. 11 is entirely due to the temperature dependence of $\rho_b\rho_c$. Similar to the T_2 transition we conclude that at T_1 the loss of carriers occurs on the hole FS. From the foregoing the picture that emerges is that above T_1 , R_H is negative ($n\mu_1\mu_2 > p\nu_1\nu_2$). At T_1 a gap occurs on the hole FS associated with a CDW with spanning vector¹⁴ $(0, 0.24, 0)$. The decrease in p relative to n drives R_H more negative. However, A (with the temperature dependence of the lifetime divided out) decreases smoothly before saturating instead of dropping abruptly to its sat-

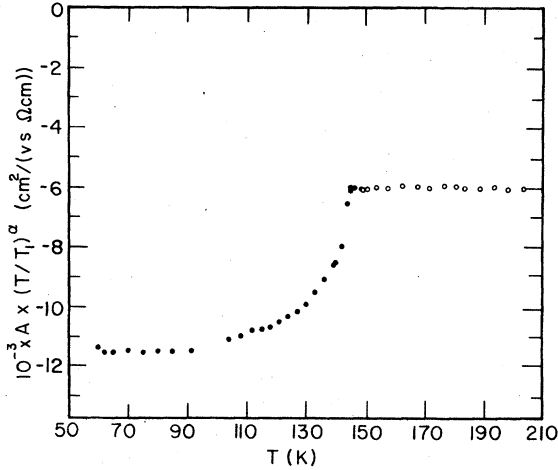


FIG. 4. Temperature dependence of $A(T/T_1)^\alpha$ around the upper transition. Below T_1 (solid circles) α equals 2.792 while above T_1 (open circles) α equals 1.774. Between ~ 100 and 145 K the steep rise in $A(T/T_1)^\alpha$ is ascribed to the thermal generation of quasiparticles across the CDW gap on the hole Fermi surface. Note that $A(T/T_1)^\alpha$ is temperature independent above T_1 and below 100 K.

uration value. This is due to the thermal excitation of quasiparticles (which are holes) across the developing gap. Below ~ 90 K these quasiparticles have been frozen out and $A(T/T_1)^{2.792}$ becomes temperature independent until T_2 where a new gap—again associated with the hole surface—appears in conjunction with a CDW of spanning vector¹⁵ (0.5, 0.26, 0.5). A is again driven to more negative values and the appearance of thermally excited quasiparticles (again holes) is shown in Fig. 3. At ~ 40 K the freeze out of these carriers is complete. No further change in carrier population occurs below 40 K. The reversal of sign of A is presumably due to the steady increase of the hole mobility versus the electron mobility at low temperatures. This picture is borne out by the analysis presented in II.

Figure 5 presents the transverse magnetoresistance data at low magnetic fields. We have defined the effective magnetoresistance mobility μ_M as the square root of the coefficient of B^2 in the expansion of the resistivity in a Taylor's series,

$$\rho(B) = \rho(0)(1 + \mu_M^2 B^2 + \dots). \quad (9)$$

Figure 5 shows the temperature dependence of μ_M in log-log scale. The striking feature of the data, in view of the model sketched above, is the monotonic power-law decrease of μ_M as T_2 is approached from below. Significantly, whereas $|R_H|$ and $\rho_b \rho_c$ attain a maximum before decreasing to their

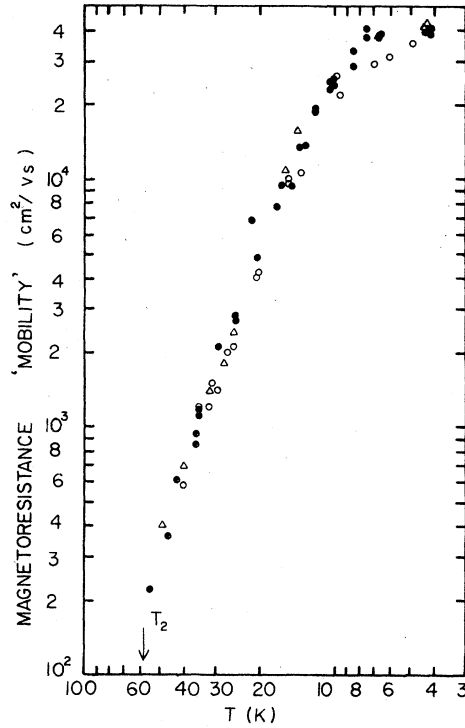


FIG. 5. Transverse magnetoresistance expressed as an effective mobility μ_M vs temperature in log-log scale [see Eq. (9)]. Data from three samples are shown. Note that the mobility μ_M continues to decrease with increasing temperature between 40 and 58 K whereas the longitudinal conductivity is rapidly rising in this temperature interval. This implies a steep increase in carrier concentration as discussed in the text.

value at T_2 , μ_M shows no such structure. Insofar as μ_M measures the lifetime of the carriers (in an averaged way) this immediately implies that the steep rise in conductivity in both b and c directions as the temperature increases from 40 K to T_2 is *not* due to any increase in carrier lifetimes. Taken together with the change in carrier concentration shown by the data on A , the data in Fig. 5 give strong support to the conventional picture of FS gapping at a CDW transition.

IV. CONCLUSION

The first measurements on the transverse dc resistivity of a transition-metal trichalcogenide are presented. Although the linear-chain crystal structure of NbSe_3 suggests the possibility of quasi-one-dimensional behavior the measured anisotropy (~ 20) is several orders of magnitude smaller than the best one-dimensional conductors. Nonetheless, the peculiar transport properties of this metal make it directly relevant to

the issues of interest in the field of highly anisotropic conductors, particularly the question of the depinning of the CDW condensate and the sliding Fröhlich mode. Some clarification of the electronic instabilities have been obtained by studying the conductivity anisotropy in relation to the Hall constant and transverse magnetoresistance. In particular it is demonstrated that the gapping occurs on the hole FS at both transitions. Furthermore, the giant resistivity anomalies in the longitudinal resistivity are shown to be a consequence of loss of carriers at T_1 and T_2 due to the slow freeze-out of thermally excited quasiparticles across a developing gap. This confirms the previously published¹³ analysis of the non-Ohmic data which also showed that the decrease in conductivity was consistent with carrier freeze-out across a gap which could be described by the BCS equation. In particular, by combining the product $\rho_b \rho_c$ with previously pub-

lished¹¹ data on the zero-field Hall constant $R_H(0)$ which shows a surprisingly large change at T_1 and T_2 we obtain an expression which shows more transparently the decrease in the hole concentration below T_1 and T_2 . Finally, the transverse magnetoresistance provides complementary information on the averaged lifetime of the carriers and shows explicitly that the resistivity anomaly at T_2 is not due to pathological changes in carrier mobilities, as has been suggested by other workers.²⁴

ACKNOWLEDGMENT

We are grateful to J. Savage for sample preparation work and Dr. J. C. Woo for help with the measurements. This work was supported by a grant from the Office of Naval Research No. N00014-77-C-0473.

-
- ¹J. A. Wilson, F. J. DiSalvo, and S. Mahajan, *Adv. Phys.* **24**, 117 (1975).
- ²W. L. McMillan, *Phys. Rev. B* **14**, 1496 (1976).
- ³S. K. Chan and V. Heine, *J. Phys. F* **3**, 795 (1973).
- ⁴A. Meerschaut and J. Rouxel, *J. Less Common Metals* **39**, 197 (1975).
- ⁵P. Haen, P. Monceau, B. Tissier, G. Waysand, A. Meerschaut, P. Molinie, and J. Rouxel, *Proceedings of the Fourteenth International Conference on Low Temperature Physics* (North-Holland, Amsterdam, 1975), Vol. 5, p. 445.
- ⁶J. Rijnsdorp and F. Jellinek, *J. Solid State Chem.* (to be published).
- ⁷T. Sambongi, K. Tsutsumi, Y. Shiozaki, M. Yamamoto, K. Yamaya, and Y. Abe, *Solid State Commun.* **22**, 729 (1977).
- ⁸T. Sambongi, M. Yamamoto, K. Tsutsumi, Y. Shiozaki, K. Yamaya, and Y. Abe, *J. Phys. Soc. Jpn. Lett.* **42**, 1421 (1977).
- ⁹A review appears in *One-Dimensional Conductors*, edited by H. G. Shuster (Springer-Verlag, Berlin, 1975).
- ¹⁰J. Chaussy, P. Haen, J. C. Lasjaunais, P. Monceau, G. Waysand, A. Waintal, A. Meerschaut, P. Molinie, and J. Rouxel, *Solid State Commun.* **20**, 759 (1976).
- ¹¹N. P. Ong and P. Monceau, *Solid State Commun.* **26**, 487 (1978). The c axis is mislabeled as the a axis in this reference.
- ¹²J. W. Brill and N. P. Ong, *Solid State Commun.* **25**, 1075 (1978).
- ¹³N. P. Ong, *Phys. Rev. B* **17**, 3243 (1978).
- ¹⁴T. Tsutsumi, T. Takagaki, M. Yamamoto, Y. Shiozaki, M. Ido, and T. Sambongi, *Phys. Rev. Lett.* **39**, 1675 (1977).
- ¹⁵R. M. Fleming, D. E. Moncton, and D. B. McWhan, *Bull. Am. Phys. Soc.* **23**, 425 (1978).
- ¹⁶S. Nakamura, and R. Aoki, *Solid State Commun.* **27**, 151 (1978).
- ¹⁷P. Monceau, N. P. Ong, A. M. Portis, A. Meerschaut, and J. Rouxel, *Phys. Rev. Lett.* **37**, 602 (1976).
- ¹⁸N. P. Ong and P. Monceau, *Phys. Rev. B* **16**, 3443 (1977).
- ¹⁹P. A. Lee, T. M. Rice, and P. W. Anderson, *Solid State Commun.* **14**, 703 (1974).
- ²⁰D. Allender, J. W. Bray, and J. Bardeen, *Phys. Rev. B* **9**, 119 (1974).
- ²¹J. Bardeen, "Recent Developments and Comments," in *Highly Conducting One-Dimensional Solids*, edited by J. T. Devresse (Plenum, New York, to be published).
- ²²N. P. Ong, *Phys. Rev. B* **18**, 5272 (1978) (following paper, referred to as II).
- ²³P. Monceau, *Solid State Commun.* **24**, 331 (1977).
- ²⁴R. M. Fleming, J. A. Polo, and R. V. Coleman, *Phys. Rev. B* **17**, 1634 (1978).
- ²⁵P. Monceau and A. Briggs, *J. Phys. C* **11**, L465 (1978).
- ²⁶H. C. Montgomery, *J. Appl. Phys.* **42**, 2971 (1971).
- ²⁷L. B. Coleman, *Rev. Sci. Instrum.* **46**, 1125 (1975).
- ²⁸B. F. Logan, S. O. Rice, and R. F. Wick, *J. Appl. Phys.* **42**, 2975 (1971).